4. T. N. Lin, "Physical theory of plasticity," in: Problems of the Theory of Plasticity [Russian translation], Vol. 7, Mir, Moscow (1976).
5. Zahn and Van, "Transition from the ductility properties of single crystals to the ductile behavior of a polycrystal in pure tension and the effect of multiple slip," Am. Soc. Mech. Eng. Trans., 106, No. 4 (1984).
6. R. Honeycombe, Plastic Deformation of Metals, St. Martin, New York (1968).
7. O. A. Volokhovskaya and V. V. Podalkov, "Elastoplastic behavior of a material with allowance for microscopic inhomogeneity," Zh. Prikl. Mekh. Tekh. Fiz., No. 6 (1981).
8. O. A. Volokhovskaya and V. V. Podalkov, "Microstresses and initial boundary of plasticity in a polycrystalline material," Izv. Vyssh. Uchebn. Zaved. Mashinostr., No. 10 (1977).
9. A. N. Mokhel', R. L. Solganik, and S. A. Khristianovich, "Theoretical description of the lag in the plastic deformation of steels," in: Plastic Deformation and Fracture of Solids [in Russian], Nauka, Moscow (1988).
10. N. N. Kudryashov, B. A. Rychkov, and Yu. N. Shvaiko, "Theoretical and experimental study of laws governing the deformation of aluminum alloy AK-6 under complex loading," Izv. Akad. Nauk KirgSSR, No. 1 (1970).
11. N. N. Mitrokhin and Yu. I. Yagi, "Systematic character of deviations from plasticity laws," Dokl. Akad. Nauk SSSR, 135, No. 4 (1960).

DYNAMIC DAMAGE AND FRACTURE OF A PLATE WITH THE EXPANSION OF A GAS CAVITY IN WATER

S. P. Kiselev and A. P. Trunev

UDC 539.3

A large number of studies (see [1], for example) have examined the fracture of a plate by pressure created in water by a gas bubble. The studies conducted thus far have generally dealt with explosive loads. In the present investigation, we examine low pressures in the bubble ($\Delta p \gtrsim 10^5$ Pa) which are created when gas is discharged from a high-pressure chamber. There are actually no small parameters in the problem in this cae, and study of the plate's fracture requires allowance for the effect of the plate on the expanding bubble, the character of discharge from the chamber, the stress–strain state of the plate, and damage accumulation in the plate.

1. Formulation of the Problem. We will examine a plate of thickness h lying on the surface of a liquid of semiinfinite depth (Fig. 1). A gas cavity located at the depth H begins to expand at a certain moment of time. The excess pressure Δp causes the plate to deform and crack, resulting in the formation of a hole of radius r^*. This very complex problem will be analyzed in two stages. First we study a linear model of the deformation of an infinite plate. The solution of this problem gives us the pressure distribution on the surface of the plate p(r, t). In the second stage, we use p(r, t) to calculate the fracture of a plate of finite dimensions with allowance for nonlinear strains.

Let us state the main assumptions underlying the given model: 1) the material remains elastic until fracture; 2) the characteristic length of the wave in the plate is much greater than its thickness; 3) the liquid is incompressible and ideal and the flow is a potential flow; 4) the gas cavity is spherical.

Given these assumptions, the equations of the liquid, with boundary conditions for the plate and the bubble, have the form

$$\Delta\varphi = 0 \quad \text{at} \quad z < 0, \quad \frac{\partial\zeta}{\partial t} + \frac{\partial\zeta}{\partial r}\frac{\partial\varphi}{\partial r} + \frac{1}{r^2}\frac{\partial\zeta}{\partial\alpha}\frac{\partial\varphi}{\partial\alpha} = \frac{\partial\varphi}{\partial z} \quad \text{at} \quad z = \zeta,$$

$$\rho\frac{\partial\varphi}{\partial t} + \rho\frac{v^2}{2} + \rho g\zeta + D\Delta_\perp^2\zeta + \rho_w h\frac{\partial^2\zeta}{\partial t^2} = 0 \quad \text{at} \quad z = \zeta, \quad \frac{\partial\varphi}{\partial r} = u_0\cos\theta + \dot{a} \qquad (1.1)$$

$$\text{at} \quad R = a,$$

Novosibirsk. Translated from Zhurnal Prikladnoi Mekhaniki i Tekhnicheskoi Fiziki, No. 5, pp. 154-158, September-October, 1991. Original article submitted January 17, 1990.

 0021-8944/91/3205-0802$12.50

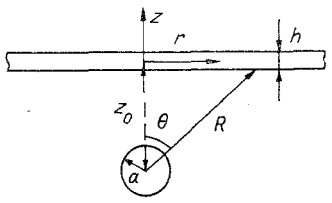

Fig. 1

where φ is the flow potential; $v = \nabla\varphi$ is the velocity of the liquid; ζ is the deviation of the plate from its equilibrium position; r, z, and α are the radial and axial coordinates and the polar angle in the coordinate system connected with the plate; ρ is the density of the liquid; ρ_w, h are the density and thickness of the plate; D is the cylindrical stiffness of the plate; g is acceleration due to gravity; R and θ are the radial coordinate and the azimuthal angle in the spherical coordinate system; a is the radius of the bubble; $\dot{a}$ is the rate of its expansion (growth); u_0 is the rate of displacement of the center of the bubble; $\Delta_\perp$ is an operator: $\Delta_\perp = (\partial/\partial r^2) + (1/r)(\partial/\partial r) + (1/r^2)(\partial^2/\partial\alpha^2)$. The following conditions for a quiescent medium are valid at large distances from the bubble:

$$\zeta \to 0,\ \partial\zeta/\partial t \to 0 \text{ at } r \to \infty,\ \varphi \to 0 \text{ at } R \to \infty,\ z = 0. \tag{1.2}$$

The initial conditions for the problem:

$$\varphi = \zeta = \partial\zeta/\partial t = 0 \text{ at } t = 0. \tag{1.3}$$

Up to the moment of fracture, the damage to the material will be described on the basis of an impulse criterion having the form [2]

$$\frac{dw_s}{dt} = \begin{cases} \nu_0 (\sigma_m/\sigma_* - 1), & \sigma_m > \sigma_*, \\ 0, & \sigma_m < \sigma_*. \end{cases} \tag{1.4}$$

Here, w_s is the damage to the medium; σ^* and ν_0 are fracture parameters; $\sigma_m = (1/3) \times (\sigma_1 + \sigma_2)$ is a normal tensile stress. In the case of axial symmetry, we have the following on the top surface of the plate when it buckles

$$\sigma_1 = -\frac{Eh}{2(1-\nu^2)}\left(\frac{\partial^2\zeta}{\partial r^2} + \frac{\nu}{r}\frac{\partial\zeta}{\partial r}\right),\quad \sigma_2 = -\frac{Eh}{2(1-\nu^2)}\left(\nu\frac{\partial^2\zeta}{\partial r^2} + \frac{\partial\zeta}{\partial r}\right) \tag{1.5}$$

(E is the Young's modulus and ν is the Poisson's ratio). Here, the fracture region is a cylinder whose radius is determined from the equation

$$w_s(r^*, t) = 1. \tag{1.6}$$

Let us now formulate the law governing the expansion of gases in the bubble. Assuming the pressure to be uniform over the volume of the cavity, we obtain

$$dp_{bu}/dt = \gamma_{bu}(\dot{m}/m - \dot{V}_{bu}/V_{bu})p_{bu},$$
$$\gamma_{bu} = \begin{cases} \gamma - \text{with adiabatic expansion}, \\ 1 - \text{with isothermal expansion}, \end{cases} \tag{1.7}$$

where p_{bu} is the pressure in the bubble; V_{bu} is the volume of the bubble; m is the mass of the gas; γ is the adiabatic exponent; $\dot{m}$ is determined from the system of equations that models the discharge of gas from a high-pressure chamber having a finite volume V_{ch}:

$$m = G,\ V_{ch}\,dp_{ch}/dt = -\gamma p_{ch}G/\rho_{ch},\ (V_{ch}/T_{ch})\,dT_{ch}/dt = -(\gamma-1)G/\rho_{ch},$$
$$V_{ch}\,d\rho_{ch}/dt = -G,$$
$$G = FB_1 p_{ch}/\sqrt{RT_{ch}} \text{ at } p_{ch}/p_{bu} > ((\gamma+1)/2)^{\gamma/(\gamma-1)},$$
$$G = FB_2 p_{ch}/\sqrt{RT_{ch}}\sqrt{(p_{bu}/p_{ch})^{2/\gamma} - (p_{bu}/p_{ch})^{\gamma/(\gamma-1)}},$$
$$B_1 = \sqrt{\gamma}\left(\frac{2}{\gamma+1}\right)^{\beta},\quad B_2 = \sqrt{\frac{2\gamma}{\gamma+1}},\quad \beta = \frac{\gamma+1}{2(\gamma-1)}. \tag{1.8}$$

Here, p_{ch}, T_{ch}, and ρ_{ch} are the pressure, temperature, and density of the gas in the high-pressure chamber; G is the rate of flow of gas from the chamber into the bubble; F is the cross-sectional area; R is the universal gas constant.

2. Solution at the First Stage. Bubble Dynamics. We represent the potential of the liquid flow in the form $\varphi = \varphi_1 + \varphi_2$, where φ_1 is the potential of the flow created by the bubble around the rigid wall; φ_2 is the potential of the flow induced by vibrations of the plate in the absence of the bubble. Linearizing boundary conditions (1.1), we write the following system of equations to determine φ_1 and φ_2:

$$\Delta\varphi_1 = 0,\ \partial\varphi_1/\partial z = 0 \text{ at } z = 0,$$
$$\partial\varphi_1/\partial R = u_0\cos\theta + \dot{a} \text{ at } R = a; \tag{2.1}$$

$$\Delta\varphi_2 = 0,\quad \partial\zeta/\partial t = \partial\varphi_2/\partial z \text{ at } z = \zeta,\quad \rho\partial\varphi_2/\partial t + \rho g\zeta + D\Delta_\perp^2\zeta + \rho_w h\partial^2\zeta/\partial t^2 = p_1,$$
$$p_1 = -\rho\partial\varphi_1/\partial t - \rho v_1^2/2. \tag{2.2}$$

The solution of problem (2.1) is already known and has the form [3-5]

$$\varphi_1 = a^2\dot{a}(1/r_a + 1/r_b) + (a^3/2)\left(u_0 + \xi^2(\dot{a} + \xi u_0)\right)\times$$
$$\times\left(P_1(\cos\theta_a)/r_a^2 + P_1(\cos\theta_b)/r_b^2\right) + (2/3)\,a^4\xi^3(\dot{a} + (2/3)\,\xi u_0)\times$$
$$\times\left(P_2(\cos\theta_a)/r_a^3 + P_2(\cos\theta_b)/r_b^3\right),$$
$$P_1(x) = x,\quad P_2(x) = (3x^2 - 1)/2,$$
$$r_a = \sqrt{r^2 + (z - z_0)^2},\quad r_b = \sqrt{r^2 + (z + z_0)^2},$$
$$\cos\theta_a = (z - z_0)/r_a,\quad \cos\theta_b = (z + z_0)/r_b,$$
$$dp_z/dt = \partial L/\partial z_0,\quad \partial p_a/\partial t = \partial L/\partial a,$$
$$\frac{dz_0}{dt} = \frac{T_2p_z + T_3p_a}{2\pi\rho a^3\left(T_1T_2 - T_3^2\right)},\quad \frac{da}{dt} = \frac{T_3p_z + T_1p_a}{2\pi\rho a^3\left(T_1T_2 - T_3^2\right)},$$
$$L = T - (4/3)\,\pi\rho a^3(p_h - p_p),\quad p_h = p_\infty + \rho g z_0,$$
$$T = 2\pi\rho a^3\left(T_1u_0^2 + T_2\dot{a}^2 - 2T_3u_0\dot{a}\right). \tag{2.3}$$

Here, p_z and p_a are generalized momenta; $\xi = a/2z_0$; z_0 is the z-coordinate of the center of the bubble; T and L are the kinetic energy and Lagrangian function of the bubble; T_1, T_2, and T_3 are coefficients of the apparent additional masses of the bubble. These coefficients are dependent on ξ and were evaluated in [3, 4]. The initial data for system (2.3) was assigned in the form

$$a(0) = a_0,\ z_0(0) = H,\ \dot{a}(0) = u_0 = 0. \tag{2.4}$$

System of dynamical equations (2.2) was integrated numerically by a Runge–Kutta method of fourth-order accuracy.

The solution of linear (relative to φ_2, ζ) system (2.2) can be represented through Fourier transforms

$$\zeta = \int_0^\infty k\,dk\sum_{n=0}^\infty e^{in\alpha}J_n(kr)\,\eta(k, n, t),$$
$$\varphi_2 = \int_0^\infty e^{kz}k\,dk\sum_{n=0}^\infty e^{in\alpha}J_n(kr)\,\Phi_2(k, n, t) \tag{2.5}$$

(η and Φ_2 are the corresponding Fourier transforms; J_n is a Bessel function of order n). In the case of axial symmetry (n = 0), we have the following simple equations for η and Φ_2

$$d\eta/dt = k\Phi_2,\quad d^2\eta/dt^2 + \omega_{ch}^2\eta = \bar{p}_1k/(\rho + \rho_w kh),$$
$$\omega_{ch}^2 = (\rho gk + Dk^4)/(\rho + \rho_w kh),\ \bar{p}_1 = \int_0^\infty p_1(r, t)\,J_0(kr)\,r\,dr \tag{2.6}$$

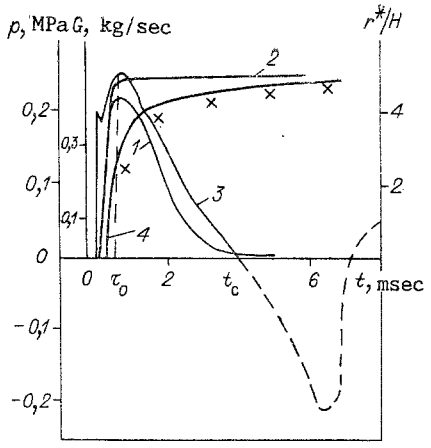

Fig. 2

with the initial conditions $\eta(0) = d\eta(0)/dt = 0$. In calculating the transform of excess pressure $\bar{p}_1$, we isolated the singular part ~1/r and transformed it independently by means of the formula

$$\int_0^\infty \frac{J_0(kr)\,rdr}{\sqrt{z_0^2+r^2}} = \frac{e^{-kz_0}}{k}.$$

The remaining part was transformed on a grid with N nodes by means of Gregory's formulas (with fifth-order accuracy). After discretization of the transform parameter on the grid at N nodes, system (2.2), (2.6) was transformed to 2N equations written in normal Cauchy form. These equations were subsequently integrated by the Runge–Kutta method. We found the functions $\zeta(r, t)$ by performing numerical integration on a grid with M nodes by means of Gregory's formulas (fifth-order accuracy). Numerical experiments established that the greatest accuracy is achieved when M = N. Due to the rapid convergence of the method, good accuracy can be attained in the given case even when N = 10.

Figure 2 shows results of typical calculations. Curves 1 and 2 show two characteristic relations G(t), curve 3 shows pressure at the center of the plate p(t), and curve 4 shows the radius of the first damage zone. Curve 1 describes G(t) for a high-pressure chamber of finite volume, while curve 2 describes the same for a chamber of infinite volume. The relation p(t) corresponds to curve 1 and is similar for curves 1 and 2 (this applies only to the initial, unsteady stage of bubble expansion; the relations p(t) are of course different during the quasisteady stage of expansion in the given case). It follows from Fig. 2 that at $t > t_c$ pressure becomes negative, which corresponds to a disturbance of continuity and vanishing of the pressure acting on the plate. Thus, it has been established that the pressure on the plate during the nonsteady stage can be considered triangular, with the same parameters as exist for a point source:

$$p(r, t) = \frac{p_m \Psi(t)}{\sqrt{1 + r^2/H^2}}, \quad \Psi(t) = \begin{cases} t/t_1, & 0 \leqslant t \leqslant t_1, \\ \dfrac{t_2 - t}{t_2 - t_1}, & t_1 < t < t_2, \\ 0, & t > t_2, \end{cases}$$

$$t_1 \approx 1{,}25\tau_0, \quad t_2 \approx t_c, \quad p_m = 0{,}5H^{-1}\tau_0^{-1/5}\rho^{2/5}(G_0RT_b)^{3/5}(1 - 1{,}95A),$$

$$t_c = 1{,}78\tau_0^{0{,}045}H^{1{,}58}(\rho/G_0RT_b)^{0{,}315}, \quad A = p_H\tau_0^{4/5}\rho^{-3/5}(G_0RT_b)^{-2/5}, \quad p_H = p_\infty + \rho gH \tag{2.7}$$

τ_0 is the time of establishment of the flow rate G_0; T_b is the temperature of the liquid; A is the back-pressure parameter.

3. Solution at the Second Stage. Plate Fracture. We will examine a plate of thickness h and radius R with a free edge. We will assume that the bottom surface of the plate is subjected to a pressure created by the expansion of the bubble. This pressure is determined from (2.7). The pressure deforms and cracks the plate and forms a circular hole of radius r*. Nonlinear Kármán equations [6] are used to describe these processes in the plate:

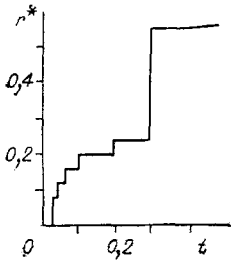

Fig. 3

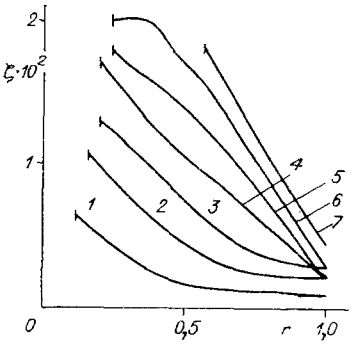

Fig. 4

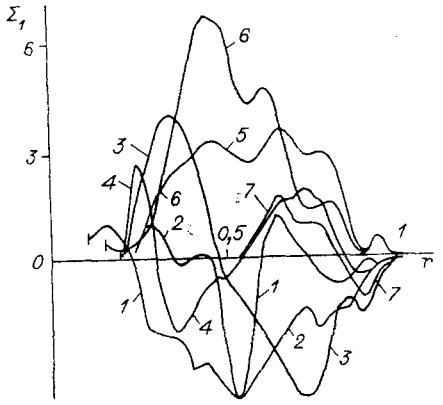

Fig. 5

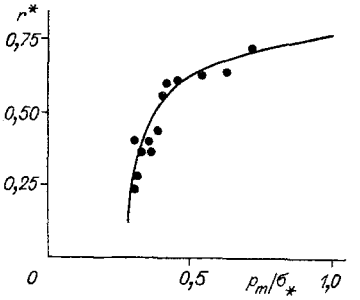

Fig. 6

$$\frac{\partial^2\zeta}{\partial t^2} = -D\Delta^2\zeta + \sigma_1\frac{\partial^2\zeta}{\partial r^2} + \left(\frac{\partial\sigma_1}{\partial r} + \frac{\sigma_1}{r}\right)\frac{\partial\zeta}{\partial r} + pR/h,$$

$$\Delta^2\zeta = \frac{\partial^4\zeta}{\partial r^4} + \frac{2}{r}\frac{\partial^3\zeta}{\partial r^3} - \frac{1}{r^2}\frac{\partial^2\zeta}{\partial r^2} + \frac{1}{r^3}\frac{\partial\zeta}{\partial r}, \quad \frac{\partial^2 u_1}{\partial t^2} = \frac{\partial\sigma_1}{\partial r} + \frac{\sigma_1 - \sigma_2}{r},$$

$$e_1 = \frac{\partial u_1}{\partial r} + \frac{1}{2}\left(\frac{\partial\zeta}{\partial r}\right)^2, \quad e_2 = \frac{u_1}{r}, \quad \sigma_1 = \frac{E}{(1-\nu^2)}(e_1 + \nu e_2), \quad \sigma_2 = \frac{E}{(1-\nu^2)}(e_2 + \nu e_1),$$

$$\Sigma_1 = \sigma_1 - \frac{E}{1-\nu^2}\frac{h}{2}\left(\frac{\partial^2\zeta}{\partial r^2} + \frac{\nu}{r}\frac{\partial\zeta}{\partial r}\right), \quad \Sigma_2 = \sigma_2 - \frac{E}{1-\nu^2}\frac{h}{2}\left(\frac{1}{r}\frac{\partial\zeta}{\partial r} + \nu\frac{\partial^2\zeta}{\partial r^2}\right) \tag{3.1}$$

(Σ_1 and Σ_2 are the total stresses on the surface of the plate). System (3.1) is written in dimensionless form. The relationships between the dimensional and dimensionless quantities are given by the formulas

$$D = D_{bu}/\left(\rho c_0^2 R^2 h\right), \quad \zeta = \zeta_{bu}/R, \quad t = t_{bu}/T, \quad T = R/c_0, \quad \sigma_i = \sigma_{i\,bu}/\bar{p}_0,$$
$$E = E_{bu}/\bar{p}_0, \quad \bar{p}_0 = \rho c_0^2, \quad D_{bu} = Eh^3/12(1-\nu^2), \quad c_0 = \sqrt{\frac{E}{3\rho(1-\nu^2)}}.$$

The damage accumulation process is described by Eq. (1.4), in which we replace σ_i with Σ_i. Assuming that the edges of the plate are free, we write the boundary conditions as

$$\left.\frac{\partial^2\zeta}{\partial r^2}\right|_{r=R} + \left.\frac{\nu}{R}\frac{\partial\zeta}{\partial r}\right|_{r=R} = 0, \left.\left(\frac{\partial^3\zeta}{\partial r^3} + \frac{1}{r}\frac{\partial^2\zeta}{\partial r^2} - \frac{1}{r^2}\frac{\partial\zeta}{\partial r}\right)\right|_{r=R} = 0, \quad \sigma_1|_{r=0} = 0. \tag{3.2}$$

It follows from the condition of symmetry that at the center of the plate

$$u_1|_{r=0} = 0, \ \partial\zeta/\partial r|_{r=0} = 0, \ \partial^3\zeta/\partial r^3|_{r=0} = 0. \tag{3.3}$$

The condition of the free boundary (3.2) exists after fracture of the plate at the point r*. System (3.1), with boundary conditions (3.2)-(3.3), was solved numerically by an

explicit "cross" scheme. Here, the order of the approximation $O[\tau^2, (\Delta h)^2]$, where τ and Δh are the steps for t and r. The calculations were performed with the dimensionless plate parameters: $h = 2\cdot10^{-2}$, $D = 0.25$, $E = 6.7\cdot10^3$, $\rho = 1$, $\nu = 0.325$. The pressure on the plate surface was determined by Eq. (2.7) with $t_1 = 10^{-3}$, $t_2 = 2\cdot10^{-2}$, $H = 5\cdot10^{-2}$, $p_m = 1.1$. Free-boundary condition (3.2) existed after fracture of the plate at point r^*.

Figure 3 shows the calculated dependence of the radius of fracture on time $r^*(t)$ [a similar relation $r^*(t)$ was seen for all values of p_m and t_2 at which the finite plate fractured]. Comparing this relation with $r^*(t)$ for the infinite plate (curve 4 in Fig. 2), we see one important difference: after the curve $r^*(t)$ reaches saturation, one more fracture occurs — and this fracture has a significantly larger radius r^* (Fig. 3). This suggests that the last fracture is different in nature from the fractures preceding it. Let us look at the fracture mechanism in greater detail. After the action of the pressure pulse, the plate begins to move upward. Since the velocity of the plate w rapidly decreases with an increase in r, bending stresses develop in the plate. These stresses become maximal at $r \approx H$. The first fracture occurs in this region. If the velocity of the particles of the remaining portion of the plate ($r^* < r < R$) is high enough, then a stress greater than the critical stress will again develop after a certain amount of time and the next fracture will occur (Fig. 4, where the plate is shown at several moments of time t_1-t_7, with $t_1 = \Delta t = 4.2\cdot10^{-2}$, $\Delta t = t_i - t_{i-1}$). After several fractures, this process ends at a certain r^*. However, along with the tensile energy in the plate, there is a substantial reserve of compressive energy. After the compression waves reach the free edge of the plate, they are reflected in the form of rarefaction waves (Fig. 5, which shows the relations $\Sigma_1(r)$ at the moments t_1-t_7). It is evident that at $t \approx t_4$ a wave is reflected from the free edge. Interference of the reflected tension waves leads to a significant increase in Σ_1. This in turn leads to another fracture at a point where $\Sigma_1 > \sigma^*$. The explanation just given is supported by Fig. 4, which shows that the curvature of the plate surface changes sign upon reflection of the wave from the free edge.

To study the dependence of r^* on p_m, we performed a series of calculations. The results are shown in Fig. 6. As noted above, the minimum value of r^* is equal to H, while the rapid increase in $r^*(p_m/\sigma^*)$ on the initial section is connected with interference effects. The fact that the curve $r^*(p_m/\sigma^*)$ forms an asymptote can be attributed to the free edge of the plate, where unloading makes it difficult to develop the tensile stress necessary for fracture. Proceeding on the basis of the equality of the kinetic energy K to the bending energy $\mathcal{E}$ we estimate the minimum value of p_m at which fracture begins. Ignoring the stresses present during the action of the pressure pulse $t < t_2$, we obtain $w = (1/2)pt_2/\rho h$. We then use this to find the relative velocity of two points separated by the distance Δr: $\Delta w = -0.5pt_2 r\Delta r/(H^2 + r^2)$. Since fracture occurs at $r \approx \Delta r \approx H$, we obtain $|\Delta w| \approx (1/\sqrt{24})p_m t_2/\rho h$, while the kinetic energy — undergoing transformation into tensile elastic energy — has the form $K \approx (\rho h/2)(\Delta w)^2 \approx (p_m t_2)^2/(4^3\rho h)$. In accordance with [6], we evaluate the bending energy from the formula $\mathcal{E} \approx (Eh^3/24)(\partial^2\zeta/\partial r^2)^2$.

We use the equality $K = \mathcal{E}$ to find the curvature $(\partial^2\zeta/\partial r^2)^* \approx (3/8)p_m t_2/(\sqrt{E\rho}h^2)$. Assuming that fracture occurs at $\sigma^* \approx (1/3)\Sigma_1 \approx (E/6)h(\partial^2\zeta/\partial r^2)^*$, we obtain the sought formula $(p_m/\sigma^*)_{min} \approx 16h/t_2c$, $c = \sqrt{E/\rho}$. Inserting the dimensionless parameters that we used into this formula, we have $(p_m/\sigma^*)_{min} \approx 0.2$. This estimate is satisfactory and agrees well with the value $(p_m/\sigma^*)_{min} \approx 0.28$ obtained in the numerical calculations (see Fig. 6).

In conclusion, we thank A. Bekker for his assistance in performing certain calculations.

LITERATURE CITED

1. Sh. U. Galiev, Nonlinear Waves in Finite Continua [in Russian], Naukova Dumka, Kiev (1988).
2. A. P. Trunev and V. M. Fomin, "Continuum model of shock erosion," Zh. Prikl. Mekh. Tekh. Fiz., No. 6 (1985).
3. O. V. Voinov, "Motion of two spheres in an ideal fluid," Prikl. Mat. Mekh., 33, No. 4 (1969).
4. O. V. Voinov and A. G. Petrov, "Motion of a sphere of variable volume in an ideal fluid about a flat surface," Izv. Akad. Nauk SSSR Mekh. Zhidk. Gaza, No. 5 (1971).
5. A. E. Wraith and T. Kakutani, "The pressure beneath a growing rising bubble," Chem. Eng. Sci., 29, No. 1 (1974).

6. L. D. Landau and E. M. Lifshitz, Theory of Elasticity [in Russian], Nauka Moscow (1987).

PENETRATION OF A RIGID CONE INTO A PLASTIC ORTHOTROPIC HALF SPACE

A. G. Akopyan

UDC 539.374

A study is made of the rigid-plastic flow of a plastic orthotropic material as a rigid rough cone penetrates a half space at a constant speed. The material of the half space is assumed to be incompressible, ideally rigid-plastic, and subject to the Mises–Hill relations [1] for a plastic orthotropic body. We assume that the principal axes of anisotropy coincide with the axes of a spherical coordinate system whose center is the vertex of the cone. An analogous problem for an isotropic material was studied in [2]; penetration of a rigid wedge into an anisotropic half space was considered in [3]; and the imbedding of a rigid stamp into an anisotropic plastic medium was investigated in [4]. A study of the penetration of a thin solid body into a transversally isotropic medium was given in [5]. In [6] a study was made of the penetration of a rigid cylindrical body into a plastic anisotropic pipe.

In the present paper we determine the pressure force during penetration of a rigid cone into a plastic orthotropic half space; we find the zone of distribution of plastic deformations and the form of the free surface of the displaced portion of half space material. A numerical example is presented showing the essential effect of anisotropy on the plastic zone distribution.

1. Assume that a rigid cone penetrates into a half space. We assume that the plastic region that is formed around the rigid cone of angle $\theta = \alpha$ is bounded by a conical surface with angle $\theta = \beta$; the location of this surface is to be determined in the course of solving our problem (Fig. 1). We assume that the region of plastic flow is bounded by a surface $r = R(\theta)$, free from external loads, whose shape is also to be determined. In this region properties of the material are assumed to be plastic orthotropic, being a consequence of plastic deformation of the material (deformation anisotropy). On the contacting conical surface there arises a tangential stress whose value depends mainly on the roughness of this surface.

Since there is no rotation of the rigid cone about its axis or the lateral area of the cone is ideally smooth in the peripheral direction, the annular component of the rate of displacement is equal to zero, whence $\gamma_{r\varphi} = \gamma_{\theta\varphi} = 0$, $\tau_{r\varphi} = \tau_{\theta\varphi} = 0$.

The differential equations of equilibrium in the spherical coordinate system then has the following form for our problem:

$$\frac{\partial \sigma_r}{\partial r} + \frac{1}{r}\frac{\partial \tau_{r\theta}}{\partial \theta} + \frac{1}{r}(2\sigma_r - \sigma_\theta - \sigma_\varphi + \tau_{r\theta}\operatorname{ctg}\theta) = 0,$$
$$\frac{\partial \tau_{r\theta}}{\partial r} + \frac{1}{r}\frac{\partial \sigma_\theta}{\partial \theta} + \frac{1}{r}[(\sigma_\theta - \sigma_\varphi)\operatorname{ctg}\theta + 3\tau_{r\theta}] = 0. \qquad (1.1)$$

Relations between the components of the deformation rate tensor, displacement rates, and stresses are:

$$\varepsilon_r = \frac{\partial u}{\partial r} = \Omega[H_0(\sigma_r - \sigma_\theta) + G_0(\sigma_r - \sigma_\varphi)],$$
$$\varepsilon_\theta = \frac{u}{r} + \frac{1}{r}\frac{\partial v}{\partial \theta} = \Omega[F_0(\sigma_\theta - \sigma_\varphi) + H_0(\sigma_\theta - \sigma_r)],$$

Erevan. Translated from Zhurnal Prikladnoi Mekhaniki i Tekhnicheskoi Fiziki, No. 5, pp. 159-163, September-October, 1991. Original article submitted September 29, 1989; revision submitted April 25, 1990.

 0021-8944/91/3205-0808$12.50